ARTIFICIAL NEURAL FUZZY BASED MPPT FOR HIGH GAIN ZETA CONVERTER FOR STANDALONE PV APPLICATION WITH GALVANIC ISOLATION

Mr. Gandham Srinivasa Rao
ACADEMIC DIRECTOR, ECE
SBIT, KHAMMAM
Email: gandham.ece@gmail.com

Dr.K.AmitBindaj
HOD, ECE
SBIT, KHAMMAM
Email: karpurapu.gavasj@gmail.com

Ms. P. Nagalaxmi
Asst Professor, ECE
SBIT, KHAMMAM
Email: nagalaxmi.sbit@gmail.com

Abstract- The installation of photovoltaic (PV) systems is on the rise globally because they provide the most direct connection to the power grid. It takes a lot of work for photovoltaic (PV) systems to work as intended. Therefore, with the help of the ANFIS MPPT method, this project aims to stabilize the DC-link voltage of the ZETA Converter. The suggested method employs a ZETA converter, which enhances voltage gain and decreases ripple content in the current and voltage outputs. To provide galvanic isolation, the system incorporates an isolation transformer. By separating the high-frequency converter's output from the PV system and other parts, this transformer improves safety. Protecting linked loads from electrical fault transfer is the purpose of galvanic isolation. A rectifier is used to provide a DC load with the output of the isolation transformer. The rectifier is designed to power DC loads by converting the transformer's alternating current (AC) output to direct current (DC). Using an intelligent MPPT helps stabilize the converter's output voltage, which in turn helps sustain DC-link voltage without converter distortions or ripples, and it also mitigates the intermittent nature of PV. A MATLAB simulation 2021a verifies the whole project.

1.INTRODUCTION

Decentralized power systems known as "off-grid stations" function apart from the central grid. These systems are often used in outlying regions when connecting to the main grid is either not possible or would incur excessive costs. In the event that the main grid becomes unavailable or unstable, off-grid stations are often used as an alternative power source. Renewable energy sources like solar, wind, and hydro power are often integrated with energy storage devices like batteries and backup generators at off-grid stations. During the day, or when there is enough wind or water flow, the station gets its electricity from the renewable sources; when renewable energy output is minimal, it gets its power from the energy storage devices. Electrification of rural areas, telecommunications, and mining activities are just a few of the many typical uses for off-grid stations.Developed nations have seen a surge in the installation of off-grid stations for both residential and commercial use in recent years. This is especially true in places where the cost of power from the main grid is high or where there is a desire for energy independence. The power needs of the intended use, the accessibility of alternative energy sources, and the constraints of energy storage devices must all be carefully considered throughout the planning and execution of off-grid stations. Particularly in outlying areas without easy access to repair and maintenance services, the system must also be dependable and simple to maintain.

STANDALONE POWER GENERATION

A system that is not connected to the grid is called an off-grid system. A PV system that is not linked to the main electrical grid is primarily known as an off-grid system. The ability to produce electricity and power appliances independently is the hallmark of an off-grid system, which is also known as a standalone system or small grid. Small communities may be electrified using off-grid technology. Because of the dispersed population and lack of infrastructure, off-grid electrification systems are a practical solution for nations with rural regions that lack access to grid energy. To live adequately apart from the grid or any other system is the definition of an off-grid system. Because the load's electrical demands may vary from the solar panels' output, it is necessary to store or preserve the electrical energy generated by the off-gird system's solar photovoltaic panels. A battery bank is one common means of doing this.

2.LITERATURE SURVEY

Yugeswar Reddy O et al (2023) have come up with a plan for the best way to run droop-controlled standalone DC mG that takes into account both economic and environmental factors while still maintaining small-signal stability. The major eigenvalue, which impacts system stability, and two additional goals are optimized by the suggested method. The authors provide an Eigen value-based stability study for network topologies where the buses may be linked only to dispatchable DG or constant power load (CPL). In addition, the appropriate probability characterisation was used to represent the uncertainties in the mG network variables that arise from the integration of solar PV power with load consumption. The suggested method makes use of a new swarm-based intelligent technology (the dragonfly algorithm) to optimize the droop settings. We solve a unique bi/tri-objective combination and talk about the outcomes. We used a solo 6-bus mG to prove that the suggested method can be easily adjusted to operate with any DC mG network. Additionally, in order to verify the suggested technique, time-domain simulations were conducted on a sample 3-bus DC mG.

Shatakshi Jha et al (2023) have concentrated on the difficulties connected with microgrids that are powered only by solar photovoltaics (PV), diesel generators (DG), and battery storage (BS). Power management, keeping the DG operating in the fuel efficiency zone (FEZ), and increasing the DG's load capabilities with nonlinear loads are all goals of the multi-objective and coordinate converter control system. The overall harmonic distortion of the DG current is also kept under 5% in accordance with the IEEE 519 standard. In addition, the control stops the DG from flowing negative sequence currents when there is an imbalance between the single and double phases. By controlling the MPPT/off-MPPT operation of the solar PV array, the state of charge (SOC) of the battery is likewise managed to avoid overcharging or overdischarging. The control is tested on a laboratory setup using hardware implementation. The results show that the control is effective and works well under many conditions. It also outperforms current methods.

Anuradha Tomar et al (2023) We have successfully addressed three main issues with rural standalone PV-based electrical systems by conceptualizing, designing, developing, and validating a photovoltaic (PV)-based single-phase micro inverter (SP μI). These issues include: 1) operating efficiently across a wide range of input voltage variations/irradiance; 2) keeping system efficiency within a satisfactory limit even under lightly loaded conditions; and 3) operating robustly and reliably under harsh outdoor operating conditions. This innovative dual-stage SP μI takes advantage of the advantages of an interleaved dc-dc boost converter to achieve phase-shifted harmonic cancellation at 180°, as well as the benefits of a voltage doubler circuit, which reduce the turn ratio of the transformer and flux leakage. As a result, the energy conversion efficiency is improved while the size of the magnet and Si-GaN are reduced. In addition, even under weakly loaded situations, the full-bridge converter's switching losses are reduced because to the tailored low-frequency switching and high-frequency switching in the first and second legs, respectively. The proposed SP μI outperforms a 500-W inverter per watt by 6.16 percent at 100% loading and 8.5 percent at 10% loading. It does this while reducing costs by 9.33 percent and increasing ROI by 12.23 percent.

Srimannarayana Kovvali et al (2023) this topology has more advantages in terms of less total standing voltage, switch count, cost factor, better efficiency, and the number of gate driver circuits, as well as in terms of voltage stress calculations, capacitors calculations, and losses calculations at various stages. It has also been compared with recent literature. It is possible to verify the theoretical performance by simulating it in MATLAB/Simulink and then test the findings using a prototype. Modulation indices, frequency modulation, switching frequencies, input voltages, and loads are all included in the experimental data. In conclusion, the experimental prototype of the suggested topology achieves the maximum efficiency of 96.5%. Whether it's for small-scale PV solar AC loads operating independently or as part of a larger grid integration system, high gain DC-DC front-end converters, transformer/inductorless operation, and DC-AC converters are essential. A step-up quadruple boost nine-level inverter based on the switched capacitor approach with fewer components is proposed in this research to accomplish all the aforementioned goals using renewable energy sources.

L. Qin et al (2022) have suggested a transformerless three-port converter (TPC) with high gain for use in freestanding PV systems. The third component for PV input is derived from one of the buffer capacitors, and the design and development of the TPC is based on a dual-inductor high-gain two-port converter. To provide maximum power point tracking control, load voltage management, and bidirectional energy flow at the battery port, a hybrid pulse-frequency modulation technique united with a pulse width modulation control approach is used. The suggested TPC has many desirable features, such as a compact rear-end inductor, low-cost gate driver, common ground shared by all ports, decreased voltage stressors, reduced power semiconductors, and continuous battery port current. The control approach, including design conditions, is thoroughly examined, along with the operating principle, steady-state features, and small-signal models. By creating a 300-W experimental prototype, which has a maximum efficiency of 97.7 percent, the theoretical analysis is shown to be valid.

H. Hasabelrasul et al (2022) to modify the inverter's output, we have introduced a new virtual synchronous generator (VSG) controller. Adjusting the inverter output and realizing the maximum power of the PV scheme are the two main functions of the VSG element and maximum power point tracking (MPPT) used in

this research. The new control technique was tested and verified by comprehensive MATLAB simulations run under various conditions, including fluctuations in load. Through the use of comprehensive MATLAB simulations, the system's output was assessed. Using console testing, a practical experiment was carried out for the VSG. We were unable to conduct experiments on the whole system because of the equipment shortage in the lab.

P. K. Bonthagorla et al (2022) have covered the topic of evaluating the performance of hybrid and traditional 7 × 7 PV array designs in a Matlab/Simulink environment using modeling, simulation, and various PSCs. Performance metrics such as global maximum power (GMP), voltage and currents at GMP, open and short circuit voltage and currents, fill factor, efficiency, and a number of local maximum power peaks (LMPPs) are used to assess and compare hybrid and conventional PV configurations. Improving the efficiency of solar photovoltaic (PV) systems is now their top priority. The power output of a PV system may be negatively impacted by partial shadowing conditions (PSCs), among other important considerations. There may be many peaks in the output power-voltage (P-V) characteristics caused by mismatch losses created between the shaded modules as a result of PSCs. Common designs that are greatly impacted by PSCs and result in higher mismatch power losses and more local peaks include series-parallel (SP), total-cross-tied (TCT), bridge-link (BL), honey-comb (HC), and triple-tied (TT). There are a number of hybrid PV array topologies that have been suggested as a means of mitigating PSCs. These include SP-TCT, BL-TCT, HC-TCT, and BL-HC, which stand for series-parallel: total-cross-tied.

Shashank Kurm et al (2022) have introduced an innovative multiport converter (MPC) that uses photovoltaic (PV) batteries to power independent loads. Using a current-fed dual active bridge (CF-DAB) architecture, the suggested converter is a reduced-stage power converter. It is possible to achieve a high voltage ratio and galvanic isolation using CF-DAB, all while maintaining efficiency. A modified modulation approach that lowers the average switching frequency of selected switches further minimizes switching losses. With fewer power conversion steps, the suggested converter regulates the load voltage and tracks the solar panel's maximum power point. The several stages that carry out maximum power point tracking, voltage boosting, and dc/ac conversion share components to accomplish this. The suggested MPC also includes a small-signal model for closed-loop control, which is applicable to various converters based on CF-DAB. We have built a lab prototype of the proposed MPC and tested it under several static and dynamic situations to confirm its functioning.

Praveen Kumar Bonthagorla et al (2022) have shown a PV array, which can be either connected to the grid or used independently, is made up of a number of PV modules that are linked together in various ways. The capacity of the PV array to generate electricity is mostly impacted by partial shadowing conditions (PSC). The PV array's power output is drastically diminished and PV module mismatching losses are caused by PSCs. Tracking the global maximum power point (GMPP) becomes very challenging when these difficulties are severe enough to cause the power-voltage (P-V) curve to exhibit several peaks. Modeling and simulating the series (S), series-parallel (SP), bridge-link (BL), honey-comb (HC), total-cross-tied (TCT), and suggested triple-tied (TT) solar PV array designs under different partial shadowing conditions is the major purpose of this research work. All PV systems are tested using a standard method that takes eight distinct shading circumstances into account. We examine the efficiency, mismatching power losses, fill factors, GMPPs, LMPPs, open circuit voltage, short circuit currents, and voltages and currents at GMPPs to evaluate the performance of the PV designs under consideration. The KC-200GT module specifications are taken into account while modeling and simulating the aforementioned PV systems in a Matlab/Simulink environment.

Niraja Swaminathan et al (2022) have suggested a fixed-zone perturb and observe (FZPO) method for photovoltaic (PV) systems that uses no extra sensors and improves steady-state efficiency while simultaneously providing rapid and drift-free maximum power point tracking (MPPT). This method involves segmenting the power-voltage (P-V) curves of the PV array into several zones, each with its own border voltages that are set for certain irradiance levels. This method uses both fixed and adjustable step sizes to boost speed; the former is determined by solving a few basic mathematical equations, which reduces the computing load. Furthermore, current methods are outdone because spontaneous drift-free tracking is accomplished without extra sampling or processing. Using just low-cost processors is made feasible by the FZPO approach, which only needs PV panel information during the initial design stage and not during real-time tracking. Hardware investigations on a buck-boost full-bridge (BBFB) converter under different irradiance circumstances demonstrate the FZPO technique's performance according to the EN50530 standard. Experimental verification shows that the FZPO methodology outperforms the traditional and VSS methods for a step change in irradiance by 42% and 20%, respectively. The peak power loss when utilizing the FZPO approach is one-sixth of what it is when using the traditional and VSS procedures under irradiance changing circumstances. Experiments are used to delve further into practical field-related matters, such the impacts of PV panel temperature.

Aditi Atul Desai et al (2022) to maximize power extraction while minimizing mismatching loss, and have concentrated on the many options for the best PV configuration under a certain shade pattern. The modeling and analysis of several PV configurations are conducted under PSCs. These configurations include Series (S), Series Parallel (SP), Total Cross Tied (TCT), Bridge Linked (BL), Honey Comb (HC), and Alternate

Total Cross Tied - Bridge Linked (A-TCT-BL). When studying the behavior of a 6×6 PV array configuration, nine different shading patterns are taken into consideration, including center, diagonal, corner, L-shaped, short and narrow, short and wide, long and narrow, long and wide, and random. Efficiency, shading loss, fill factor, mismatching loss, open circuit voltage, short circuit current, global maximum power point (GMPP), and maximum voltage are the metrics used to compare their performances. To maximize power generation under PSCs while minimizing wiring complexity and the amount of cross ties, a new hybrid configuration termed the A-TCT-BL PV Configuration is developed. When compared to S, SP, BL, and HC PV Configurations under most of the PSCs studied, the simulation results show that this proposed configuration—which is an integration of TCT and BL PV—can generate maximum power, fill factor, efficiency, and minimum mismatching loss. The simulation is conducted using Matlab/Simulink software and takes into account a Canadian Solar CS5P-200M PV module.

Rohini Sharma et al (2022) have shown an ESOGI-FLL-WIF control algorithm that is robust, improved, and second-order generalized integrator. This algorithm is used to manage the voltage and frequency of a microgrid and improve power quality. With its straightforward design, rapid convergence, and top-notch dynamic and steady-state responsiveness, this control is a real find. To evaluate the essential component from dc bias contaminated current and harmonics, the ESOGI-FLL-WIF control method is used. When things are fleeting, the ESOGI-FLL-WIF control approach keeps tabs on the frequency and adjusts accordingly. To provide a level playing field, the ESOGI-FLL-WIF control algorithm's performance is evaluated in contrast to that of pre-existing controls. A solar photovoltaic array and a synchronous reluctance generator (SyRG) operated by pico-hydro turbines make up this three-phase, four-wire island system. Due to its great efficiency and lack of permanent magnets in the rotor, SyRG is a cost-effective alternative to traditional generators. While the system incorporates battery energy storage for active power management, the four-leg converter adjusts neutral current and manages reactive power injection during unbalance load conditions. In order to ensure the control strategy's efficacy and feasibility, a system prototype is created and tested under various load unbalancing and solar insolation change scenarios.

H. U. R. Habib et al (2021) have concentrated on discovering the best ways to utilize biomass, taking into account particular uses for biogenerators (BGs) using BG-PV-WT-BSS and BG-PV-SMES based freestanding rural MG systems. The first BG-PV-WT-BSS case study used the improved-MILP (I-MILP) method to suggest the best size and selection of DGs for a rural MG. Lowering total net present cost (TNPC), levelized cost of energy (LCOE), and greenhouse gas emissions were the aims of this research. As for the second scenario, BG-PV-SMES, it is a concept for a rural microgrid that incorporates photovoltaics and a variable speed bio generator (VSBG). Then, in the rural MGs, a streamlined EMS was developed in the MATLAB/Simulink ® environment to coordinate the operation control of the DERs. The simplified EMS suggests coordinated control based on FOSMC and FCS-MPC for DGs linked via power converter. A power converter based on FOSMC and FCS-MPC is designed to enhance system performance, including power quality, regulated voltage, and total harmonic distortion (THD), even when subjected to external disturbances. The simulation results demonstrate that FOSMC and FCS-MPC perform better with lower total harmonic distortion (THD) and higher power quality.

Chittaranjan Pradhan et al (2021) have developed a hybrid maximum power point tracking (MPPT) algorithm that uses the perturb and observe (P&O) method with modified invasive weed optimization (MIWO) to efficiently extract the maximum power from a freestanding PV-based hybrid system in situations with partial shade and fast weather change. To quickly get the worldwide peak and maximum PV power, MIWO applies the P&O algorithm in the latter stages of MPPT after handling the earlier stages. Included in the microgrid under investigation are the following components: PV system, load, battery, electrolyzer, and fuel cell. To prevent the battery from being subjected to damaging charging and discharging operations, the hybrid microgrid's subsystems work together to adopt a coordinated approach for power management and dc-voltage control. The dc/dc converter connected to the battery and dc link also functions as the PV's MPPT circuit when dc voltage is monitored, eliminating the need for a separate specialized circuit. The voltage oscillations of the microgrid are reduced or eliminated when the Takagi-Sugeno (TS) fuzzy controller is used to manage the power demand and solar irradiance. It is evident from the data that the suggested approach outperforms several of the current strategies.

Anjeet Verma et al (2021) a three-phase electric vehicle charging station (EVCS) that incorporates a solar photovoltaic (PV) array and a storage battery to enhance grid power quality; this system makes use of a convex combination affine projection sign algorithm (APSA). The results of two APSAs, one with a big step size and the other with a tiny step size, are convexly combined using this approach. As a result, even when input circumstances are subject to sudden changes, this method converges quickly and has a small steady-state error. Because the charging current of an EV fluctuates often, this method is suited for an EVCS. Charge your electric vehicle with either AC or DC power with the EVCS. While it's daylight, the CS charges the EV linked at the PCI by running in standalone mode. A bidirectional dc-dc converter, however, allows the dc-powered EV to draw power from the dc connection. In contrast, the CS draws electricity from the grid when PV array

production is not available. The smooth mode transition is also accomplished by synchronizing the PCI voltage with the grid voltage when the CS is connected to the grid. The experimental prototype has been subjected to a battery of tests in both steady-state and dynamic conditions to prove that it behaves as expected.

Rahmat Khezri et al (2021) have created a new method for demand side management (DSM) that takes into account the ideal dimensions of a home's solar photovoltaic (PV), wind turbine (WT), and battery storage (BS). Battery charge status and predicted solar radiation and wind speed for the next day form the basis of the DSM approach. At its heart, the DSM is a fuzzy logic approach that determines the most effective ways to move or reduce loads. Both the DSM approach and the operational reserve take into account the day-ahead predicting mistakes generated using an artificial neural network method. The Rain flow counting technique is used to determine the deterioration of the battery's capacity in order to get a realistic model of the battery and to predict its lifespan. This research uses a typical South Australian (SA) home as its case study. The suggested technique optimizes three distinct power supply system configurations: PV-BS, WT-BS, and PV-WT-BS. Both with and without the suggested DSM method, the PV-WT-BS system proves to be the optimal configuration for achieving the lowest power costs. The suggested strategy is very efficient in reducing power cost without emissions, according to a comparison of the best-case scenario findings with an existing system in South Africa and two newly published publications.

Rishi Kant Sharma et al (2021) established a hierarchical control system for the PV-BES-DG system that relies on dc integration at a shared dc bus, using dc droops. Compared to its alternating current (ac) equivalent, the dc integration allows for greater management of the hybrid system and removes PV's scaling constraint. To further guarantee optimum load sharing across DG and BES, an ideal secondary control based on regulators is suggested. In addition, a power management scheme (PMS) is developed to guarantee the standalone system's dependable operation in the event of power imbalances between the source and the load, as well as during operation in the critical state of charge limit condition of the BES. Beyond a certain low-level loading, the PMS also limits DG operation. In order to further understand how droop and optimum regulator gain impact the stability of the system, a small signal stability study is introduced. The suggested PMS and hierarchical control of the PV-BES-DG system based on dc droop is tested in a laboratory-scale prototype.

Muhammad Najwan Hamidi et al (2021) A 31-level asymmetrical switch-diode based multi-level DC-link (MLDCL) inverter is suggested to include a capacitor compensator (CC) circuit and a perturb and observe (P&O) based voltage regulator (POVR). To implement MLDCL in a freestanding PV system, which requires consistent DC voltages from the panels, the POVR method is used to control the voltage and ensure that the system can produce its maximum power while operating at full load. To facilitate the POVR functioning, boost DC-DC converters link the panels to the inverter. Regardless of changes in ambient and load circumstances, the findings demonstrate that POVR can achieve the requisite fixed DC voltages, maintaining a stable output of 230 V. An impressive 97.21% of the theoretical maximum power is delivered by the standalone system when it is fully loaded. When powering inductive loads, CC is also used to reduce voltage spikes at the output.

Sachin Jain et al (2021) have shown an easy way to handle power management and do away with the problem of switching between modes in a hybrid system that uses stand-alone photovoltaic (PV) batteries. This article provides a straightforward method for controlling voltage that works for the same purpose. To remove the need to toggle between charging and discharging modes, the provided method employs a voltage band approach. The use of the inner voltage band also removes the need to toggle between the charging and discharging modes, as well as the intermediate PV mode. Since the suggested control approach is based on data about the load voltage, it allows for the seamless transition between modes. It prolongs the battery's life by preventing the switching cycle's charging and discharging phases from overlapping. Furthermore, the power information and complicated calculations (such as division, etc.) are not necessary for the functioning of the provided control method. Maximum power point tracking (MPPT) allows for autonomous management of the battery's charging and discharging, making the provided solution simply implementable on any PV-battery-based hybrid system. In order to ensure the functioning in several modes with smooth control, a simulation was conducted. Experimental data from the constructed lab prototype further justify the simulation results.

Vahid S et al (2020) have introduced the generalized systematic method; now we will apply it to two examples and talk about the topologies that come out of it. A more thorough discussion of the several ways a TPC may function is also planned for the article. In addition, we will showcase the simulation findings and discuss how the suggested method was applied to create a new three-port power converter. One major factor is their increasing use in solar and traction applications, where they are used to combine various energy sources and storage. The literature on topology-proposed circuits (TPCs) is extensive, but there is no one-size-fits-all method for developing or designing one according to the inputs and outputs that are involved.

3.EXISTING SYSTEM

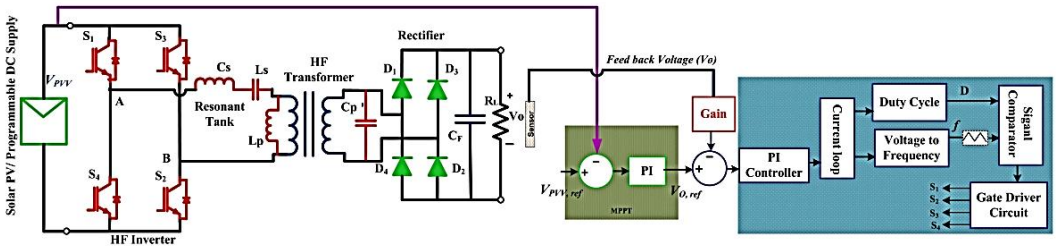

Figure: 3.1 Block diagram of PV fed MPPT-based dc–dc resonant converter

This current setup makes use of a dc-dc resonant converter with dual control as a front-end component to efficiently extract power from photovoltaic (PV) sources. Standard dc-dc boost converters often have less efficiency and more parts needed for soft-switching. Also, there is a limit to how efficiently converters transmit electricity when integrating PV. Therefore, this paper explores a suggested control scheme for an isolated dc-dc resonant converter in order to provide broader voltage regulation and optimize PV power output in order to tackle these issues. With a larger range of operational loads, this converter can even achieve zero-voltage switching. It offers a straightforward method of controlling power consumption per tub and monitoring the maximum power point, which enhances efficiency even when the load is low without affecting the precision of the digital signal processor.

In order to effectively utilize PV, regulate the upstream resonant converter's output voltage against variations in PV voltage, and sustain soft switching of the resonant converter over a wide range with narrow frequency operation, an effective control approach is needed. This approach can be achieved with general purpose digital signal processors (GSPs). To counteract the decline in converter performance caused by the restrictions imposed by duty cycle and switching frequency, this article discusses a dual control strategy. In order to achieve better voltage regulation, it is necessary to implement duty cycle control before ZVS fails. Then, in a sequential and simultaneous manner, the switching frequency and duty cycle are adjusted to automatically regulate the required output voltage across the entire load range. This ensures a wider ZVS range and narrow frequency operation. The aforementioned resonant converter topologies may work at maximum power point (MPP) with input voltages that fluctuate to a certain degree, but they can't achieve broad input line voltage regulation, which leads to inefficient system performance. Therefore, selecting a control technique, converter configuration, and integrated power utilities takes a lot of work in the design process. Consequently, this article explains how to effectively regulate the input line voltage, restrict the frequency, and modify the duty cycle of a PV-fed dc-dc converter while operating in voltage control mode utilizing a dual control approach for an MPPT algorithm. The power circuit is comprised of a dual-control-method modified LCLC series resonant converter that optimizes PV power and maintains the converter output voltage across a larger range of input power changes. The experimental findings of the 2.2 kW converter that were shown here prove that the method that was suggested works.

3.2 PV CHARGER SYSTEM OPERATING MODES

One of four possible modes of operation for the suggested PV charger system is taken into account, depending on the load power need, the state of charge of the batteries, and the available PV power. The suggested PV charge controller may run the system in one of the four modes indicated before in order to accomplish the necessary functionality.

3.2.1 MPPT - MODE

This mode allows for the immediate extraction and delivery of the maximum PV power to both the DC load and the battery. Actually, this method of operation is possible for the system under one of these two circumstances: a) - The maximum power from the PV system is less than the power needed to run the system, and the remaining power is provided by the battery without overdischarge.

3.2.2 NON - MPPT MODE

The maximum power that the battery can absorb, Pbmax, is higher than the extracted maximum PV power, PMPP, in this mode, which is also more than the needed load power, P_R. The battery might be damaged since the charging current, i_b, is greater than the maximum current, currenti_bmax, in this case. This problem may be circumvented by using a PV power limiting strategy to activate the PV array at a different point in time than the normal MPP.

3.2.3 NIGHT MODE

This mode allows the system to function when the PV array's power generation is close to nil and the battery can meet the load requirement without going into deep drain.

3.2.4 PV CHARGER AND MODEL CONTROL

This mode is activated when the power consumption per unit of load (PMPP < PR) is less than the power supply from the battery, and the remaining power demand (PR - PMPP) cannot be met, as shown. Thus, in order to prevent the battery from going into deep drain and to enable it to be charged by the available PV power, a load separation is required. The proposed control method is summarized in the flow diagram, which is based on the four operational modes that have been outlined.

3.3 PV CHARGER SMALL-SIGNAL MODEL

A buck converter small-signal model using the average variable approach is executed to get the charge control's small-signal transfer functions. The aforementioned lead-acid battery model and the linear PV model are included into this model even further. A constant voltage Vb is used to mimic the latter. Furthermore, the effects of the capacitor's equivalent series resistance (RC) and the inductor's resistive losses (RL) are not ignored in order to simplify the compensator design and to get an accurate buck converter model.
A comprehensive PV charger system average model is therefore obtained. Rather of using non-linear switching devices like transistors and diodes, a theoretical DC transformer is used. This DC transformer is characterized by an averaged model of the transistor-diode for continuous conduction mode (CCM).

3.4 DRAWBACKS OF EXISTING SYSTEM

• Variations in external factors, including temperature and sun irradiation, and the load characteristic may have a significant impact on PV power and diminish its conversion efficiency.
• Nevertheless, should a problem with the wind-up of the integral component of the PI compensator ever occur, the control performance might drastically worsen.
• The findings obtained from using the existing-MPPT approach to monitor the solar system are subpar.
• This converter exhibits large switching losses and lacks dependability when subjected to different situations.

4.PROPOSED SYSTEM

4.1 PROPOSED SYSTEM

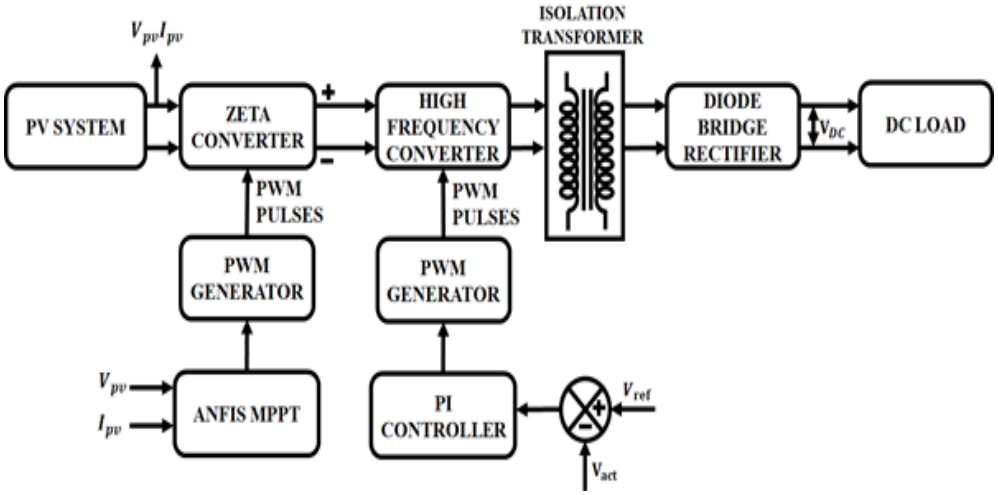

Figure: 4.1 proposed block diagram

A Zeta converter receives DC electricity from solar panels in this proposed Standalone Solar electricity System. A connection is made between the load and the converter's output.

Using an ANFIS MPPT algorithm, the system aims to optimize the power production from the solar panels. This algorithm continuously monitors the solar panels' highest power point and modifies the converter output appropriately. A high-frequency converter receives the Zeta converter's output. The voltage output of this converter is stabilized and precisely regulated by a PI controller. The high-frequency converter is an essential component in the power distribution chain since it changes the electrical power, makes it more efficient, and helps with the next steps. To provide galvanic isolation, the system incorporates an isolation transformer. By separating the high-frequency converter's output from the PV system and other parts, this transformer improves safety. Protecting linked loads from electrical fault transfer is the purpose of galvanic isolation. A rectifier is

used to provide a DC load with the output of the isolation transformer. The rectifier is designed to power DC loads by converting the transformer's alternating current (AC) output to direct current (DC).

4.2 SOLAR PV SYSTEM

Solar photovoltaics are the building blocks of a photovoltaic system, which in turn generates energy by absorbing and converting sunlight. To ensure the solar panels withstand wind, rain, hail, and rust, they should be securely fastened to a sturdy and sturdy structure. A constant angle, determined by the building's location, the local altitude, and the electrical load requirements, must be specified for the solar PV array. Because southern hemisphere orientation is directly proportional to local latitude, northern hemisphere solar modules must be pointed southward. The ground-mounted solar panels may follow the sun's optimum path by angling themselves in either a horizontal or vertical plane.While this is one efficient way, it does need additional upkeep. Arrays are collections of solar panels that have their individual panels connected in either series or parallel; the notation for this configuration is Np or Ns. The solar cell's specs allow one to determine the open circuit voltage (Voc) and short circuit current (I Sc). One way to think about the voltage and current that solar PV produces is as V PV and I PV, respectively. With the use of maximum power point tracking (MPPT), the solar PV system can extract its maximum power, as well as its peak voltage and current. Depending on the varied input temperatures and solar intensities, the solar panels generate electricity from the sun.

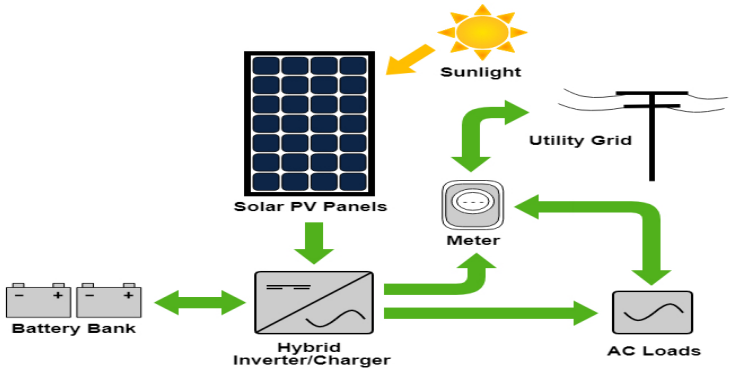

Figure: 4.2 Solar PV System connected to the grid

To get the most out of the system, which is the maximum voltage and current, the FLC-based MPPT system is supplied this power. One kind of logic controller is the field-programmable logic controller (FLC), which allows us to regulate the system's output by enforcing a predetermined set of rules. The DC-DC converter's gate pulse is based on the fuzzy logic's output, which is in turn derived from the delay angle output and sent into the PWM generator. The voltage source inverter (VSI) takes the DC output from the Landsman converter and turns it into AC voltage. The AC voltage is then sent to the AC grid. It is possible to remove AC signal harmonics by using LC filters. It is possible to get the output AC voltage from the output DC voltage using the formula Vdc = Vac / √2.

4.3 ZETA CONVERTER

You may convert the input voltage V_PV to the required output voltage V_DC with the help of a zeta converter. The voltage V_DC is compared to the reference value V_ref in order to get an error voltage. Then, the chosen controller is instructed to modify the duty ratio of the converter based on this voltage. The controller sends its output to the PWM generator, which controls the converter's switching operation by means of pulses. Using a driver circuit increases the voltage of a pulse width modulation (PWM) generator's output. Therefore, the steady-state inaccuracy in the output may be reduced by adjusting the converter's duty ratio.You can see the two capacitors C_1 and C_2, the switch MOSFET, the two inductors L_1 and L_2, the load resistor (R), and the one diode (D) that make up the zeta converter. When it comes to ON and OFF switching circumstances, the zeta converter circuit relies on CCM.

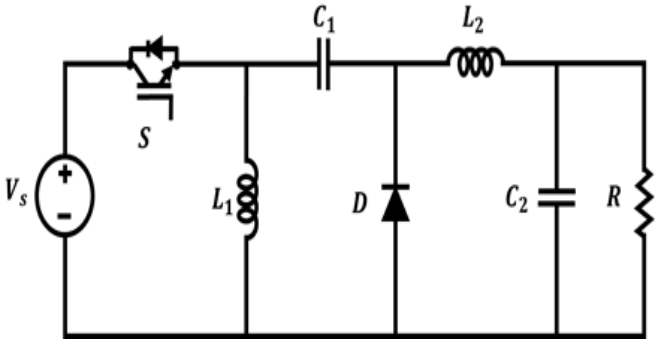

Figure: 4.3 Basic circuit diagram of Zeta Converter

Mode 1

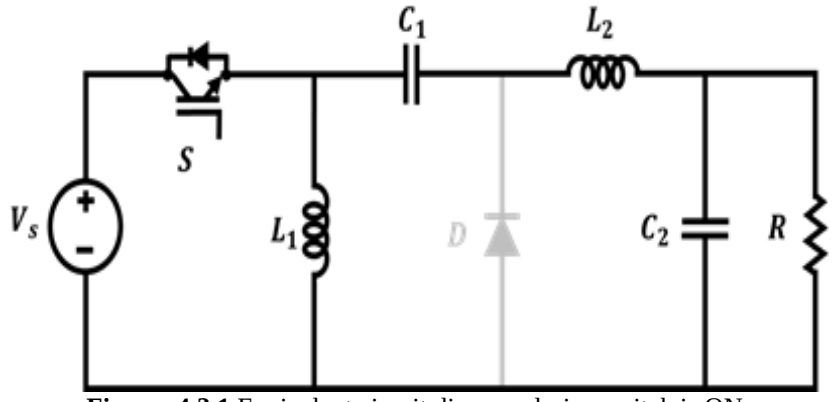

Figure: 4.3.1 Equivalent circuit diagram during switch is ON

The operation in Mode 1 is shown in Figure 4.3.1. At the ON state of the switch, current flows through the inductor, which aggregates linearly and stores energy, while the diode is reverse biased and takes current from the (Vs). A voltage that is equal to the inductor voltage is the input voltage or source voltage. At the same time, C_1 starts charging to its output voltage. The two inductors L_1, L_2 store energy from the supply and generate output current when the MOSFET is switched on.

Mode 2

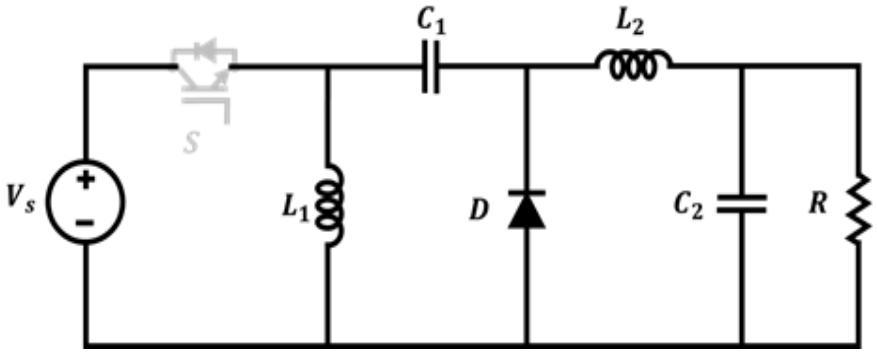

Figure: 4.3.2 Equivalent circuit diagram during switch is OFF

Mode 2 functioning is seen in Figure 4.3.2. In mode 2, the diode is forward biased, the capacitor is parallel to the L_2 inductor, and the output voltage is accessible across the inductor due to the discharge of C_1 and the charging of C_2 to the output voltage. The switch is in the "OFF" position. The load resistor will receive any energy that remains in the inductor (L).Consequently, instances involving this sort of surgery are being discharged.The Zeta converter's timing diagram is shown in Figure 4.8.

The duty cycle of Zeta converter is given in Equation (4.16)

$$D = \frac{V_O}{V_i + V_O} \qquad (4.16)$$

Assuming that the inductors used have the same amount of ripple current for both indicators L_1 and L_(2), the values of the inductors may be calculated using the following equation.

$$L_1 = L_2 = \frac{DV_{in}}{F * \Delta I} \qquad (4.17)$$

The equations for capacitors are given as follows,

$$C_1 = \frac{DV_O}{F * R\Delta V} \qquad (4.18)$$

$$C_2 = \frac{DV_{in}}{8 * F^2 * L_2 * \Delta V} \qquad (4.19)$$

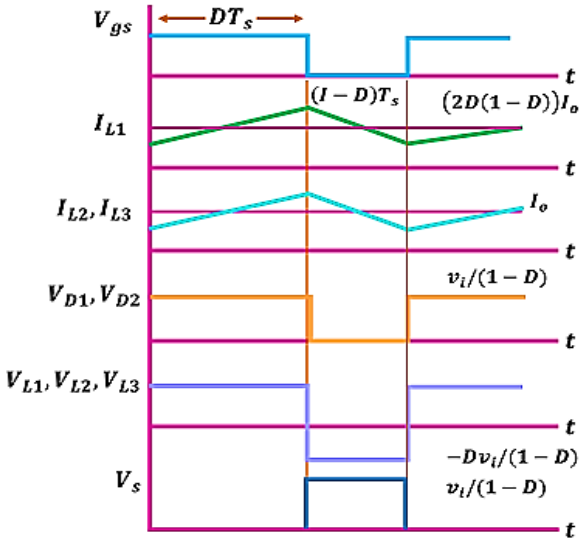

Figure: 4.3.3 Timing diagram of Zeta converter

Using a controller, we can maintain a steady output from the zeta converter. The groundbreaking ANFIS hybrid system combines the best features of Fuzzy Inference System (FIS) and Artificial Neural Networks (ANN), making it both flexible and smart.

Fuzzy rule sets, derived by the FIS from the ANN's learning abilities, help optimize parameters. In order to drive the FIS-based MPPT, the ANN is taught to assess the best MPP when the ANFIS method is used to MPPT operations. The ANFIS method is ideal and flexible for PV systems since it can handle problems caused by uncertainty and unanticipated changes very well. The ANFIS method achieves its high accuracy and rapid convergence because to its hybrid learning strategy, which incorporates both back propagation and least square approaches. It is previously known that the PV system's conversion efficiency may be improved using the ANFIS-based MPPT.

To accomplish tracking the maximum power of the PV module under changing weather circumstances, a novel approach based on ANFIS is presented for maximum power point tracking (MPPT). All three of these parameters—PV voltage, I_pv current, and T_pv cell temperature—are suggested as inputs. The duty cycle is the output variable that controls the DC-DC switching Luo converter to maintain maximum power tracking. The likelihood of attaining optimum performance is limited due to the fact that standard FLC modeling relies on trial and error. As a result, ANFIS learning may provide membership functions and fuzzy rules. It is recommended to begin by gathering the training data. Here are the procedures to acquire the training data:We used standard MPPT algorithms to model the system in a variety of temperature and solar radiation scenarios.The data were acquired and processed using a MATLAB script specifically designed for this task in order to obtain the required results.A further step was to reshuffle the altered data. In order to acquire just the unique rows in the data collection process, the results are filtered again.

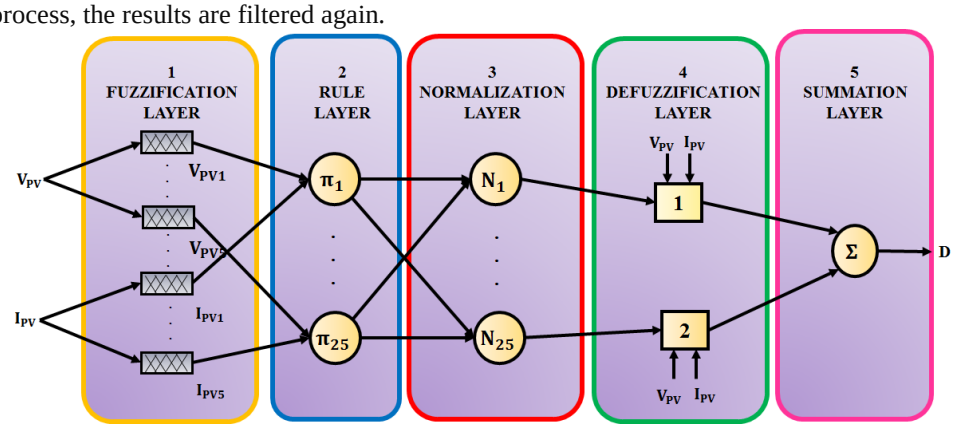

Figure: 4.11 ANFIS model structure

The V_pv, I_pv, and T_pv data sets are the input training data to the ANFIS. The five-layer network that forms the general structure of the proposed ANFIS model is shown in Figure 4.11. The ANFIS-generated PV voltage (V_pv) membership function is shown in Figure 4.12. Both the PV cell temperature (T_pv) and the PV current (I_pv) membership functions are shown in Figures 4.13 and 4.14, respectively. Low, medium, and high are the names of the three generic bell-shaped membership functions that are applied to each input. If you want to make

sure the switched boost landsman converter gets the right gate pulses, you need to check the duty cycle output with the saw tooth signal. Under varying environmental circumstances, the PV voltage changes from its original value, which is the region of the voltage at maximum power. In contrast, the area of the current at maximum power (also known as the PV current) changes under various environmental circumstances. The temperature of the PV cells may also range from 298 K to 323 K. Prior information collected from the training dataset is used by the ANFIS controller to produce the membership functions, as previously mentioned. There is some shape variation in the membership function both during training and in the final form that is produced when training is complete.

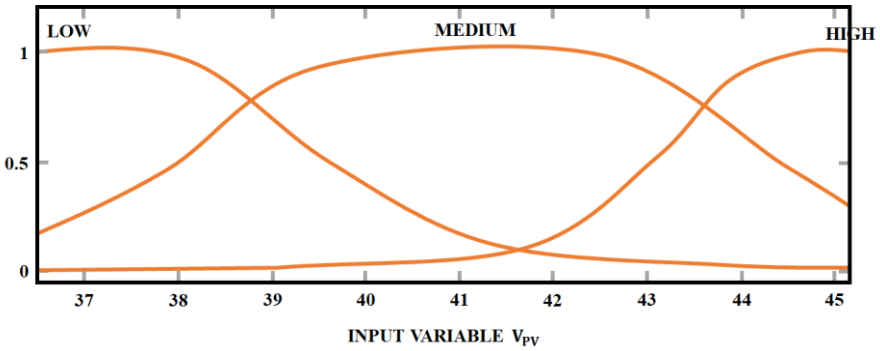

Figure: 4.12 The membership function of the input variable (V_{pv})

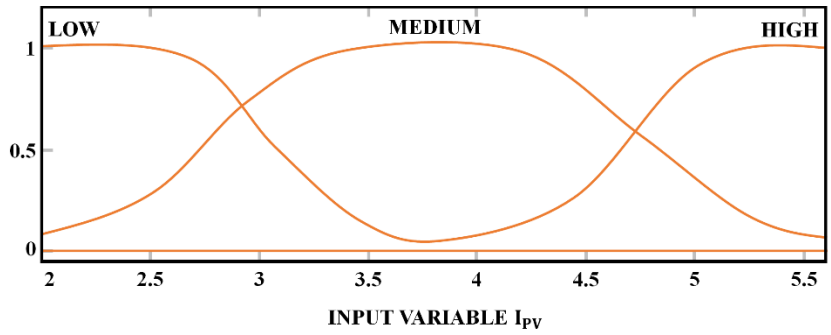

Figure: 4.13 The membership function of the input variable (I_{pv}).

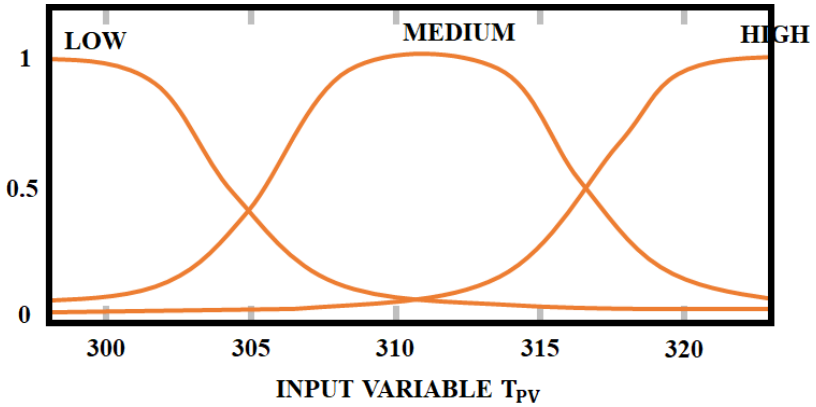

Figure: 4.14 The membership function of the input variable (T_{pv}).

Once ANFIS has been trained with enough epochs, it can create the input-output mapping for training datasets. For each given set of input values, ANFIS creates a new set of fuzzy rules by tweaking the membership functions. In order to minimize the mistake, the parameters of the membership functions are fine-tuned. The ANFIS model is prepared for use in the MPPT control scheme after all the membership function parameters have been changed. It is necessary to use checking data, which is distinct from training data, to verify the outputs of the ANFIS learning model before applying it to MPPT control. Once again, parameters of membership functions are altered to reduce error if it exceeds the required value. Placing a DC-DC switched Zeta converter between a solar PV module and the load allows for the greatest power transmission to the load via the regulation of the duty cycle of the converter.

4.4 FORWARD CONVERTER

In a typical forward converter, the coupled inductor serves as the topology, with a pulse width modulation (PWM) switch on the main side and two diodes on the secondary. In Figure 4.15, we can see an example of common forward converters. The forward converter takes a direct current (dc) input that may be either constant or variable. Diode polarity is controllable via the winding connection of a connected inductor. You may adjust the secondary side windings to suit your needs. To make the circuit easier to understand, use a continuous dc source to power it. Ideally, the switch would have a high switching frequency ("Q1"). By using MOSFETs, one may accomplish quick dynamic control over duty ratio. A voltage isolator is a connected inductor.

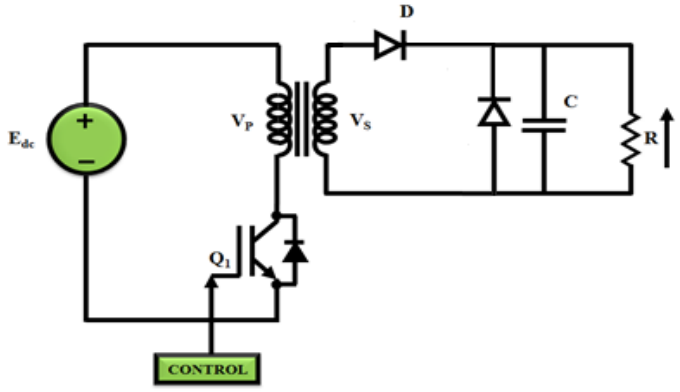

Figure: 4.4 Forward Converter

A forward converter with an efficiency of more than 95% and a conversion ratio of more than 10:1 is shown in figure 4.4. This converter makes use of a switched-diode-capacitor (SDC) stage. The single SDC stage is indicated by the red outline. The cascaded output stages of SDC lower the inductor volume, switch stress, and capacitor.

Conventional boost converters utilize a cascade of output stages; buck boost inverters sometimes make use of the MLFC (Multilevel Flying Capacitor) converter. The output is reduced by a factor of five by each of the extra three stages of SDC, which are flying capacitors Cf1 to Cf3. Flying capacitors equalize the voltage during steady-state operation, where k is the interest stage and N is the level of converters, which is (k*Vout) / (N-1). Distributing the load on the electronic system across many stages helps lower the required component voltage rating and their volume.

5.RESULT AND DISCUSSION

The following outcomes are produced by applying the suggested procedure to MATLAB simulations.

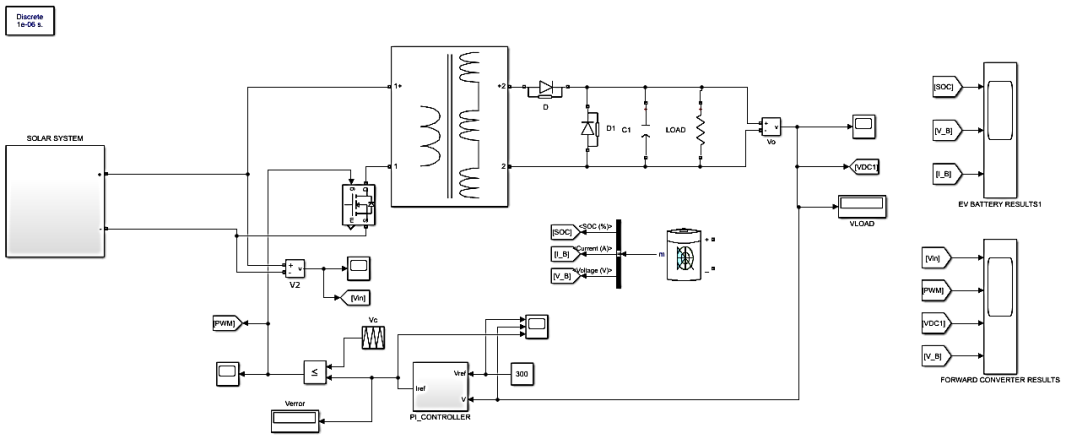

Figure: 5.1 Simulation Diagram

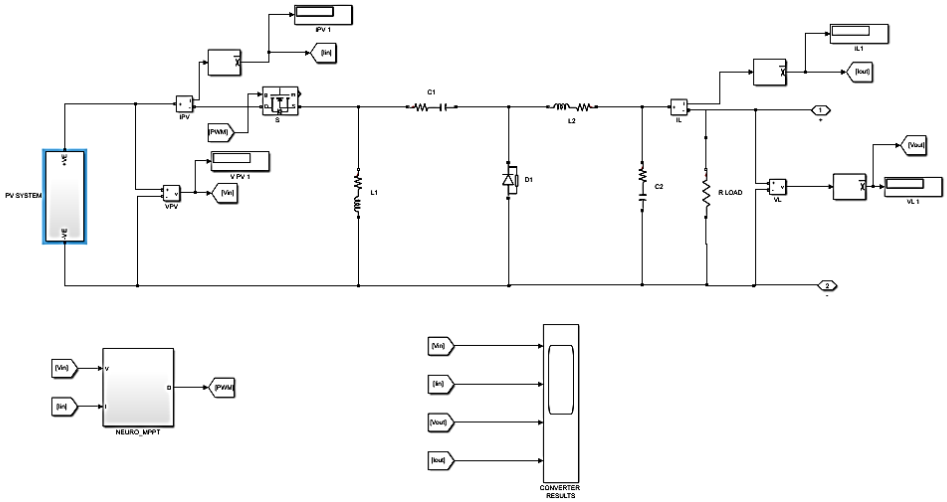

Figure: 5.2 Simulation Diagram for solar with converter

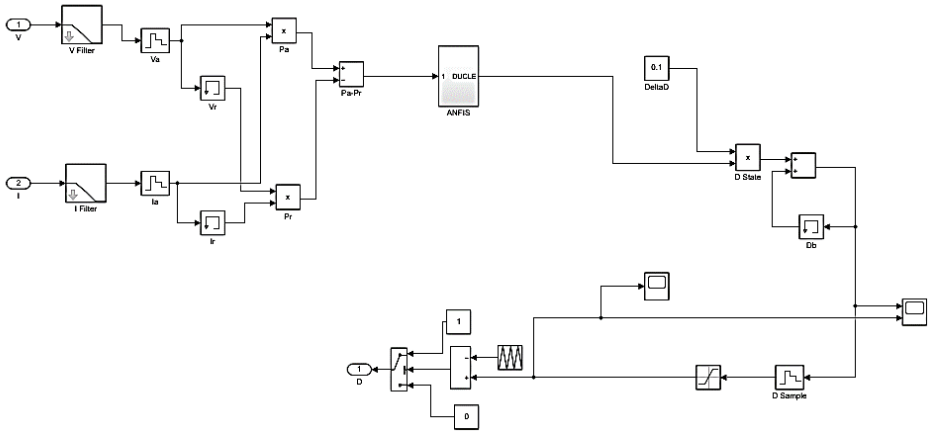

Figure: 5.3 Simulation Diagram for ANFIS MPPT

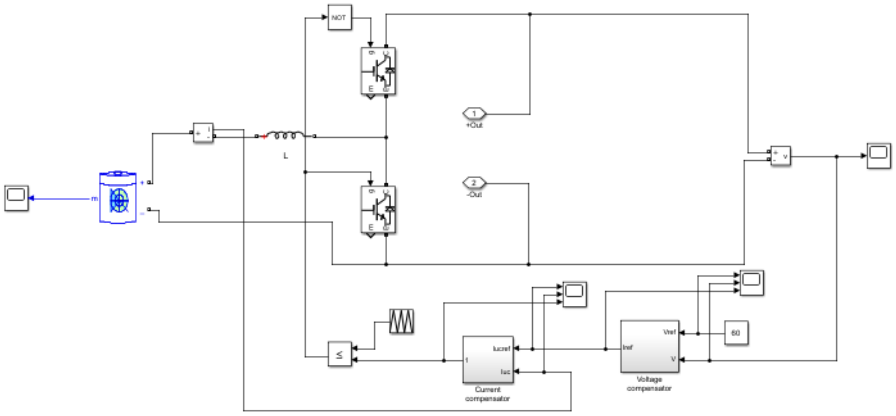

Figure: 5.4 Simulation Diagram for Battery converter

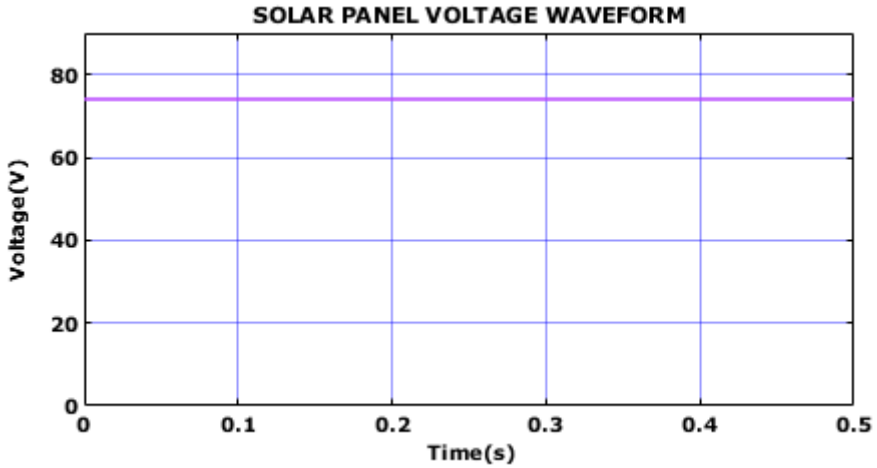

Figure: 5.5 Input voltage to the converter

The figure 5.5 represent the solar panel voltage waveform which attained an input voltage of 75V at constant temperature $35^{\delta\ \text{temperature}}$ and 1000 w^2/sq. irradiance.

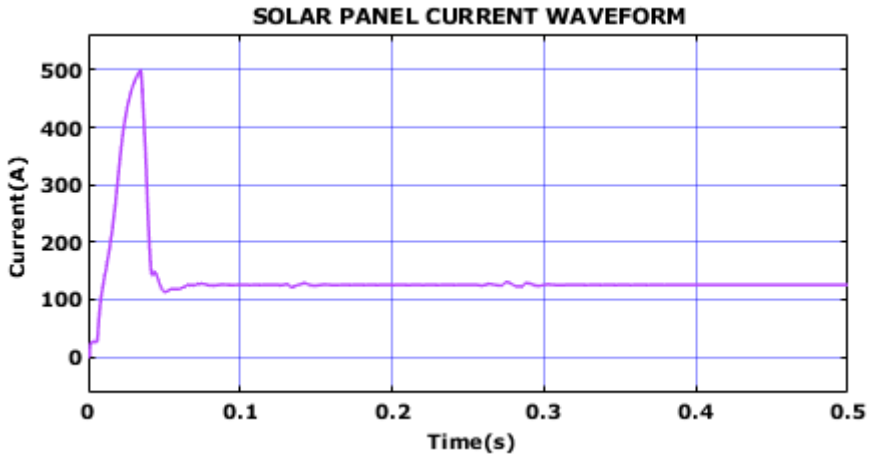

Figure: 5.6 Input current to the converter

The figure 5.6 represent the solar panel current waveform which attained an input current of 128A at constant temperature $35^{\delta\ \text{temperature}}$ and 1000 w^2/sq. irradiance.

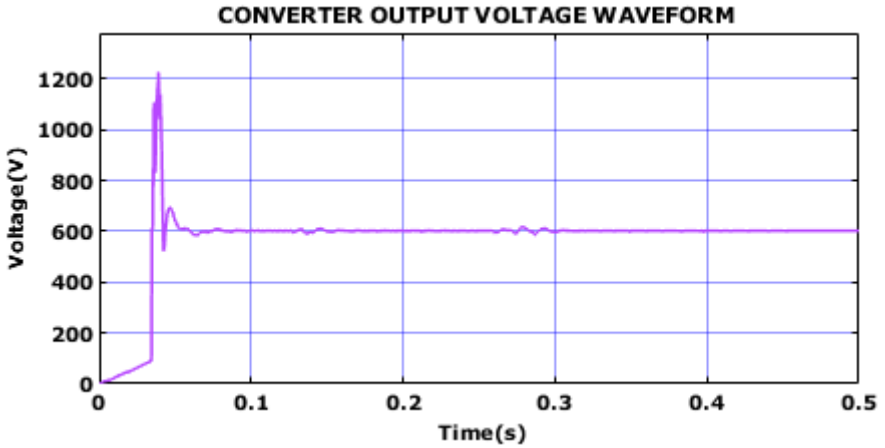

Figure: 5.7 converter output voltage

The figure 5.7 represent the converter output voltage waveform which attained a voltage of 600V at constant temperature $35^{\delta\ \text{temperature}}$ and 1000 w^2/sq. irradiance.

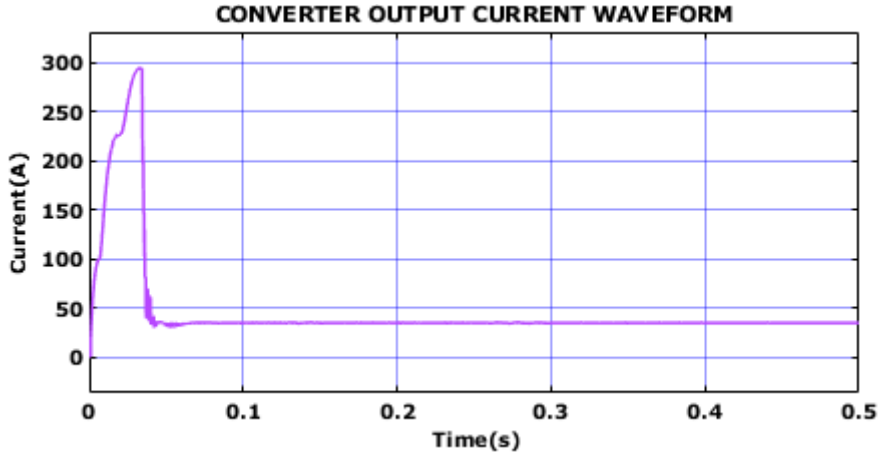

Figure: 5.8 converter output current

The figure 5.8 represent the converter current waveform which attained a current of 47A at constant temperature $35^{\delta\ \text{temperature}}$ and 1000 w^2/sq. irradiance.

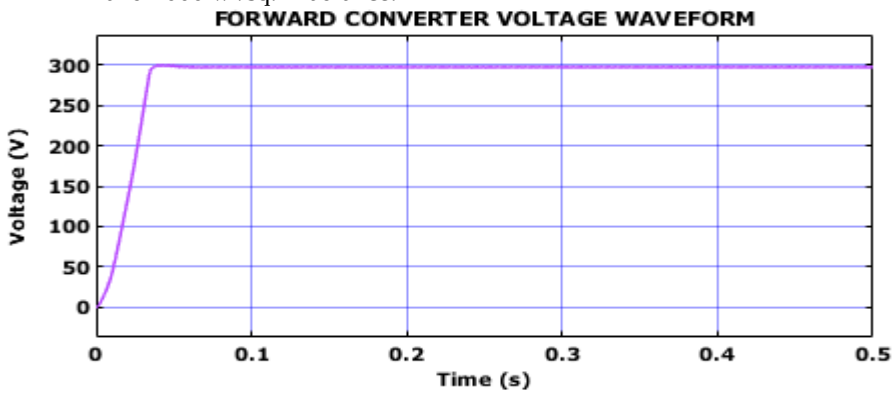

Figure: 5.9 Forward Converter

The Figure 5.9 Forward Converter represent the waveform for dc load which provide galvanic isolation for protection. The 300V produced from the converter is given to DC load as battery.

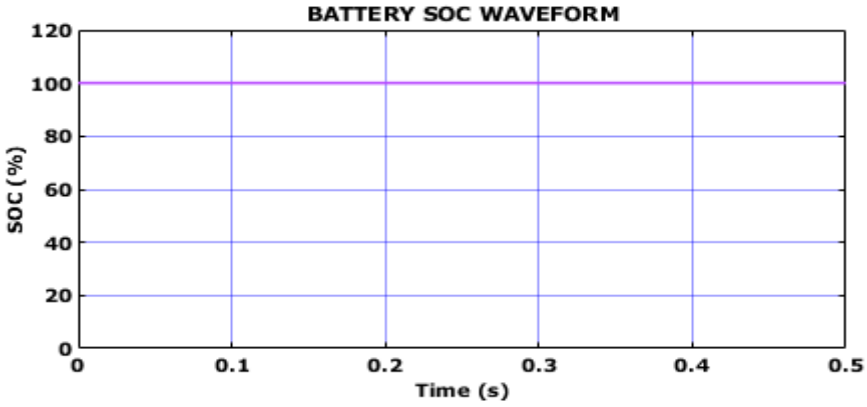

(a)

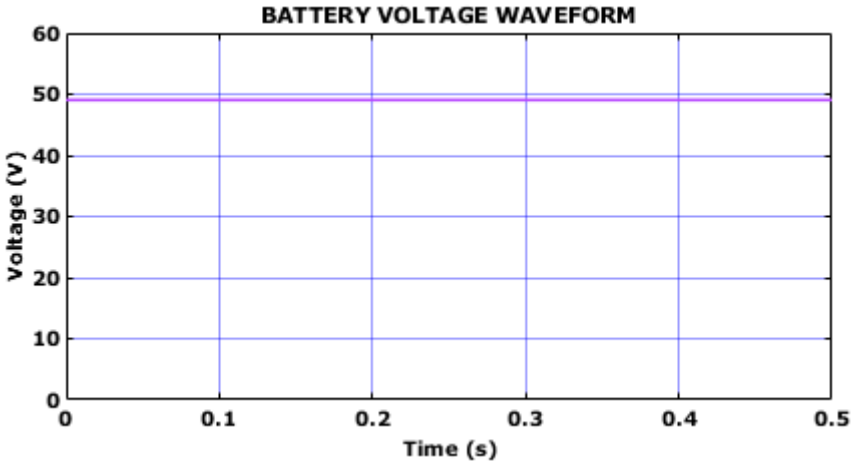

(b)

Figure: 5.10 Waveforms of battery (a) SOC and (b) Voltage

See Figure 5.10 for waveforms that show the battery voltage and state of charge. The voltage of the batteries is 12V. As shown in Figure 5.10 (b), the waveforms for the state of charge (SOC) of the battery are successfully monitored. The SOC is 60%. Using batteries, the excess electricity that is produced by the PV is stored. In the event that the main power source is down, the backup battery will deplete and provide electricity to the load.

CONCLUSION

Finally, one encouraging strategy for optimizing power production and system efficiency in off-grid solar PV applications is the use of a ZETA converter coupled with ANFIS MPPT. Having a battery source as a backup ensures that the loads will always have a steady supply of power, even when solar power isn't enough. Using the ANFIS MPPT algorithm shortens reaction times to changing weather conditions and enhances monitoring of the maximum power point. The use of state-of-the-art control methods and power electronics components is crucial to the project's goal of improving the energy conversion process's efficiency. A rectifier is used to provide a DC load with the output of the isolation transformer. The rectifier is designed to power DC loads by converting the transformer's alternating current (AC) output to direct current (DC). When used alone, the isolation transformer's galvanic isolation greatly improves the system's dependability and safety. Because of its independent operation, this system may be used in places that don't have access to the main power grid. We have successfully confirmed the findings of this project after implementing it in Matlab Simulation 2021a.

FUTURE SCOPE

In the next five years, the battery management system is predicted to see a growth of five to seven times. With a valuation of $5 billion in 2020 and optimistic projections of $35 billion by 2026, e-commerce is poised to become 15% of the global vehicle market over the next five years. Looking forward, we can see that charging technologies will undergo significant advancements.

You may expect it to resemble the refueling experience, for example. The voltage at which vehicles may be charged will rise from 500V to 800V in the coming years, and the power output of a single charger will rise from 60kW to 350kW. This translates to a practical reduction in charging time from an hour to ten or fifteen minutes.

Energy storage technologies are used. Improve the dependability of stand-alone load systems by integrating PI controllers with energy storage devices like batteries or supercapacitors. Its primary function was to regulate the energy stored in such systems, maintaining a steady flow of electricity to the load.

• Advancements in affordable system design and manufacturing: Communities requiring dependable and long-term stand-alone load solutions will be able to afford PI controllers in the future.

Interleaved converter performance may be improved by the use of sophisticated control algorithms. These methods can include adaptive control and model predictive control (MPC). Better control precision and stability may be achieved by enhancing the converter's reaction to variations in input voltage or load demand using these techniques.Connected devices would completely alter the way electric vehicles are charged. To improve charging experiences and make the most efficient use of resources, it will intelligently link grids, networks, renewable energy, batteries, and vehicles. The term "Internet of Vehicles" (IoV) would describe this setup.

There will be a dramatic uptick in the market for battery-powered transportation vehicles. Large corporations want to project an image of being ecologically conscious. Deploying zero-emission commercial cars is a part of

their present plan.

That is why EV charging companies will have to build mega-chargers to make these massive EVs usable over longer distances. The equipment that was created has been tested on a small scale in the lab, and it may be safely installed in my substations to ensure that it works as intended in a real-world setting. If the load is dynamic, automated PF correction could lead to harmonic problems due to the bank of capacitors being switched on and off so often. To prevent the frequent switching of capacitor banks, it is possible to build an optimal algorithm and a suitable filter based on the frequent load change pattern. It is possible to do a comparison analysis to determine the best spot for correctional equipment in terms of efficiency and cost-effectiveness in the field.

REFERENCES

1. Y. R. O, J. J, A. K. Chakraborty and J. M. Guerrero, "Stability Constrained Optimal Operation of Standalone DC Microgrids Considering Load and Solar PV Uncertainties," in IEEE Transactions on Power Delivery, vol. 38, no. 4, pp. 2673-2681, Aug. 2023, doi: 10.1109/TPWRD.2023.3253623.
2. S. Jha, B. Singh and S. Mishra, "Rule-Based Power Management and Quality Enhancement in a Standalone Microgrid," in IEEE Transactions on Industry Applications, vol. 59, no. 4, pp. 4484-4494, July-Aug. 2023, doi: 10.1109/TIA.2023.3261870.
3. A. Tomar, "Efficient PV-Based Microinverter With Enhanced ROI for Lower Economic Zone Habitants," in IEEE Canadian Journal of Electrical and Computer Engineering, vol. 46, no. 1, pp. 24-34, winter 2023, doi: 10.1109/ICJECE.2022.3223294.
4. S. Kovvali, N. Jayaram, S. V. K. Pulavarthi, Y. R. Shankar, J. Rajesh and V. G. Prasant, "Quadruple Boost Switched Capacitor-Based Inverter for Standalone Applications," in IEEE Access, vol. 11, pp. 30442-30458, 2023, doi: 10.1109/ACCESS.2023.3260257.
5. L. Qin et al., "Transformerless High-Gain Three-Port Converter With Low Voltage Stress and Reduced Switches for Standalone PV Systems," in IEEE Transactions on Power Electronics, vol. 37, no. 11, pp. 13468-13483, Nov. 2022, doi: 10.1109/TPEL.2022.3182309.
6. H. Hasabelrasul, Z. Cai, L. Sun, X. Suo and I. Matraji, "Two-Stage Converter Standalone PV-Battery System Based on VSG Control," in IEEE Access, vol. 10, pp. 39825-39832, 2022, doi: 10.1109/ACCESS.2022.3165664.
7. P. K. Bonthagorla and S. Mikkili, "Performance Investigation of Hybrid and Conventional PV Array Configurations for Grid-connected/Standalone PV Systems," in CSEE Journal of Power and Energy Systems, vol. 8, no. 3, pp. 682-695, May 2022, doi: 10.17775/CSEEJPES.2020.02510.
8. S. Kurm and V. Agarwal, "Dual Active Bridge Based Reduced Stage Multiport DC/AC Converter for PV-Battery Systems," in IEEE Transactions on Industry Applications, vol. 58, no. 2, pp. 2341-2351, March-April 2022, doi: 10.1109/TIA.2021.3137371.
9. P. K. Bonthagorla and S. Mikkili, "Optimal PV Array Configuration for Extracting Maximum Power Under Partial Shading Conditions by Mitigating Mismatching Power Losses," in CSEE Journal of Power and Energy Systems, vol. 8, no. 2, pp. 499-510, March 2022, doi: 10.17775/CSEEJPES.2019.02730.
10. N. Swaminathan, N. Lakshminarasamma and Y. Cao, "A Fixed Zone Perturb and Observe MPPT Technique for a Standalone Distributed PV System," in IEEE Journal of Emerging and Selected Topics in Power Electronics, vol. 10, no. 1, pp. 361-374, Feb. 2022, doi: 10.1109/JESTPE.2021.3065916.
11. A. A. Desai and S. Mikkili, "Modeling and Analysis of PV Configurations to Extract Maximum Power Under Partial Shading Conditions," in CSEE Journal of Power and Energy Systems, vol. 8, no. 6, pp. 1670-1683, November 2022, doi: 10.17775/CSEEJPES.2020.00900.
12. R. Sharma, S. Kewat and B. Singh, "Power Quality Improvement in SyRG-PV-BES-Based Standalone Microgrid Using ESOGI-FLL-WIF Control Algorithm," in IEEE Transactions on Industry Applications, vol. 58, no. 1, pp. 686-696, Jan.-Feb. 2022, doi: 10.1109/TIA.2021.3128371.
13. H. U. R. Habib et al., "Optimal Planning and EMS Design of PV Based Standalone Rural Microgrids," in IEEE Access, vol. 9, pp. 32908-32930, 2021, doi: 10.1109/ACCESS.2021.3060031.
14. C. Pradhan, M. K. Senapati, S. G. Malla, P. K. Nayak and T. Gjengedal, "Coordinated Power Management and Control of Standalone PV-Hybrid System With Modified IWO-Based MPPT," in IEEE Systems Journal, vol. 15, no. 3, pp. 3585-3596, Sept. 2021, doi: 10.1109/JSYST.2020.3020275.
15. A. Verma and B. Singh, "CAPSA Based Control for Power Quality Correction in PV Array Integrated EVCS Operating in Standalone and Grid Connected Modes," in IEEE Transactions on Industry Applications, vol. 57, no. 2, pp. 1789-1800, March-April 2021, doi: 10.1109/TIA.2020.3041812
16. R. Khezri, A. Mahmoudi and M. H. Haque, "A Demand Side Management Approach For Optimal Sizing of Standalone Renewable-Battery Systems," in IEEE Transactions on Sustainable Energy, vol. 12, no. 4, pp. 2184-2194, Oct. 2021, doi: 10.1109/TSTE.2021.3084245.

17. R. K. Sharma, S. Mudaliyar and S. Mishra, "A DC Droop-Based Optimal Dispatch Control and Power Management of Hybrid Photovoltaic-Battery and Diesel Generator Standalone AC/DC System," in IEEE Systems Journal, vol. 15, no. 2, pp. 3012-3023, June 2021, doi: 10.1109/JSYST.2020.3032887.
18. M. N. Hamidi, D. Ishak, M. A. A. M. Zainuri, C. A. Ooi and T. Tarmizi, "Asymmetrical Multi-level DC-link Inverter for PV Energy System with Perturb and Observe Based Voltage Regulator and Capacitor Compensator," in Journal of Modern Power Systems and Clean Energy, vol. 9, no. 1, pp. 199-209, January 2021.
19. S. Jain, S. Dhara and V. Agarwal, "A Voltage-Zone Based Power Management Scheme With Seamless Power Transfer Between PV-Battery for OFF-Grid Stand-Alone System," in IEEE Transactions on Industry Applications, vol. 57, no. 1, pp. 754-763, Jan.-Feb. 2021, doi: 10.1109/TIA.2020.3031265.
20. Vahid, S., & El-Refaie, A. (2020, February). Generalized systematic approach applied to design a novel three-port power converter. In 2020 IEEE International Conference on Industrial Technology (ICIT) (pp. 542-548). IEEE.